



Experimental thermal characterization of timber frame exterior wall using reed straws as heat insulation materials

Sergiu-Valeriu Georgescu¹ · Camelia Coşereanu¹ · Adriana Fotin¹ · Luminița-Maria Brenci¹ · Liviu Costiuc¹

Received: 31 October 2018 / Accepted: 27 April 2019 / Published online: 28 May 2019
© Akadémiai Kiadó, Budapest, Hungary 2019

Abstract

The research presented in this paper proposes structures of timber frame exterior walls using reed straws as insulation materials. Having thicknesses of 175 mm and designed for exterior building walls, the proposed structures are composed of 12-mm-thick oriented strand board, 150-mm-thick insulation material with and without air layers, a vapour barrier foil and 12.5-mm-thick gypsum board for the interior face of the wall. The insulation materials used as reference for the proposed structures are polystyrene and rock wool. Reed straws used as insulation material for the tested wall structures formed insulation layers of 150 mm thickness in five configurations: 150-mm loose-fill reed straws without air layer and other four variants with loose-fill reed straws and 100-, 50-, 20- and 10-mm-thick air layers, respectively. The air layer was placed at the contact with gypsum board for all configurations. The reference structures (rock wool and polystyrene as insulation materials) followed three of the configurations set-up, namely 150-mm-thick insulation material (rock wool or polystyrene) only and insulation materials with air layers thicknesses of 100 and 50 mm, respectively. The eleven tested structures were subjected to thermal conductivity coefficient (λ) measurements. The tests were performed on HFM436 Lambda equipment. The structures were tested for an entire cycle of temperatures varying between -10 and 30 °C and thus simulating summer and winter climate conditions. The thermal conductivity coefficient of the exterior walls filled with loose reed straws as insulation material was recorded between mean values of 0.076 and 0.077 $\text{W m}^{-1} \text{K}^{-1}$, except the structure with an air layer of 100 mm, for which a value of 0.120 $\text{W m}^{-1} \text{K}^{-1}$ was registered.

Keywords Wood frame · Wall structure · Thermal conductivity · Reed straws

List of symbols

λ	Thermal conductivity ($\text{W m}^{-1} \text{K}^{-1}$)
T	Temperature (°C)
ρ	Density (kg m^{-3})
ΔT	Temperature difference (°C)
T_m	Mean temperature (°C)
u	Reed moisture content (mass%)

GB	Gypsum board
VB	Vapour barrier
x	Air layer thickness

Subscripts

EPS	Polystyrene
RW	Rock wool
RS	Reed straws
OSB	Oriented strand board

Introduction

Building energy use accounts for about 40% of the total energy consumption in EU and the USA, and in European countries, the building space heating represents the most part of the energy consumption, namely 50% of the primary energy demand [1]. In this respect, building insulation materials have a major contribution to the reduction in the heating and cooling energy consumptions of buildings. Wood houses and timber frame walls filled with various thermal insulation materials play an important role in reducing the heating energy consumption level and CO_2 emissions. The comparison of different types of insulation materials should consider both the building energy

✉ Camelia Coşereanu
cboieriu@unitbv.ro

¹ Department of Wood Processing and Wood Products Design, Faculty of Wood Engineering, Transylvania University of Brasov, B-dul Eroilor 29, 500036 Brasov, Romania

consumption and CO₂ emissions [2]. Commercial building insulation materials such as polystyrene (EPS), rock wool (RW) are used largely nowadays, but have the main drawback that they negatively affect the environment, especially due to their long time necessary to biodegrade.

The sustainability concept in building design encouraged researches in developing thermal and acoustic insulators using natural materials [3]. Several researchers focused on using small wood particles or shavings [4–6] in timber frame wall structures as loose-fill materials. Wood frame wall system with spruce bark fill material [4] proved to have low thermal conductivity values between 0.062 and 0.096 W m⁻¹ K⁻¹. Other studies investigated the thermal transmittance of the building walls insulated with straw bales and reed straws as sustainable materials [7–10], recording low values of thermal transmittance for considerable thicknesses in the range of 420 to 580 mm and for the horizontally arrangement of the reed straws in the structure. Straw bales with a thickness of 50 cm proved to have low thermal conductivity of 0.067 W m⁻¹ K⁻¹ [10]. Wood frame walls with layers of paper spaced at 3, 5 and 7 mm were investigated for their heat insulation capacity, and thermal conductivity coefficients between 0.047 and 0.059 W m⁻¹ K⁻¹ were recorded. Lower thermal conductivity coefficients are obtained for the thinner air layers in the structure, due to the reduced impact of the convective heat transmittance [11]. Cellulose loose-fill material obtained from recycled paper is also studied as heat insulation material [12, 13], in wood frame wall structures registering low thermal conductivity coefficient values up to 0.050 W m⁻¹ K⁻¹ [12]. Flax and jute are also promising for this category of materials [14–16].

Thermal conductivity coefficient (λ) is one of the material's properties that characterize the heat insulation performance, and it is often used to select the appropriate material for building envelopes or thermal insulators [17]. Experimental methods of measuring λ are based on using heat flow meters with flux sensors and temperature control systems [6, 18] and in situ measurements using sensors for the determination of temperatures and relative humidity [19–21]. Experimental research is accompanied in several scientific papers by theoretical analysis using numerical methods [22] and computational models, such as finite methods [23–25]. An actual modern non-destructive method used to analyse the structures is the X-ray computed tomography which allows structure-based thermal modelling, applied by few researchers to investigate low-density bark-based panels as promising insulation materials [26].

This study presents an experimental approach to the thermal performance of timber frame exterior walls filled with reed straws as heat insulation materials and the comparison to similar structures where common insulation

materials such as rock wool (RW) and polystyrene (EPS) were used. The thermal conductivity coefficient (λ) was measured on eleven types of wall structures including the reference ones. The study includes also an investigation on the influence of the air layer thickness on the thermal conductivity coefficient values and the variation of λ as function of density (ρ). The experiment was carried out in laboratory conditions using HFM436 Lambda apparatus (Netzsch, Selb, Germany) for the measurements.

Experimental

Materials

The core of the experimental exterior walls includes three types of thermal insulation materials (Fig. 1), namely loose bulk reed straws (RSs), rock wool (RW) and expanded polystyrene (EPS). Commercial RW and EPS having thicknesses of 50 mm were used as reference to compare the thermal insulation performance of reed straws. RS had initial moisture content (u) of 11%, bulk density (ρ) of 79.43 kg m⁻³ and a measured thermal conductivity coefficient (λ) of 0.054 W m⁻¹ K⁻¹. The measured mean diameter of the reed straws was of 5 mm. RW batt (fire-proof Baudeman Izo 42 Duo-Euroclass A1) with thickness of 50 mm, density of 30 kg m⁻³ and λ of 0.04 W m⁻¹ K⁻¹ and Baudeman EPS 50 mm (fire reaction class E1, water absorption $\leq 2.5\%$, compressive strength of 50 kPa), with density of 15 kg m⁻³ and $\lambda = 0.042$ W m⁻¹ K⁻¹ were used for the experimental structures. The 12-mm-thick oriented strand board (OSB 3) was used for the exterior face sheet, and commercial 12.5-mm gypsum board (GB) was used for the interior face sheet. OSB panels had a density of 600 kg m⁻³ and a thermal conductivity coefficient (λ) of 0.125 W m⁻¹ K⁻¹, whilst the GB's density was 680 kg m⁻³ and measured λ was of 0.202 W m⁻¹ K⁻¹. An aluminium-based foil (Isoflex Alu-PZ produced by S.C. Masterplast Romania S.R.L.) with a specific mass of 55 g m⁻² was used as vapour barrier (VB).

Experimental Walls

The structures were formed as seen in Fig. 2, where (1) is the interior face sheet GB, (2) is the vapour barrier (VB), (3) represents the wall sides made from commercial 18-mm particleboard. Heat insulation materials (4) used for the experiment were RS, RW and EPS, respectively. The exterior face sheet of the experimental walls (5) shown in Fig. 2 is OSB 3. The wall frames were constituted from the particleboard sides which were connected with OSB

Fig. 1 Thermal insulation materials used for the experimental exterior walls; **a** reed straws; **b** rock wool; **c** polystyrene

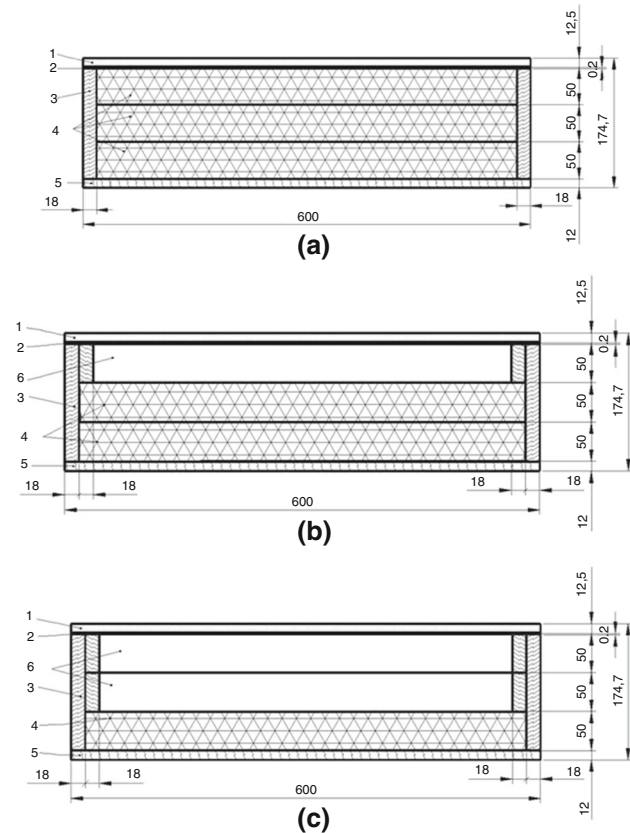
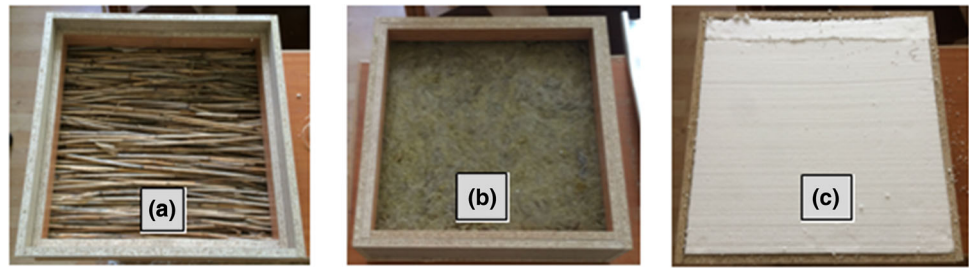


Fig. 2 Tested structures of the experimental exterior walls; **a** without air layer; **b** 50-mm air layer; **c** 100-mm air layer

exterior face sheet by screws and then filled with insulation materials.

First, the insulation materials were arranged in three layers, filling the entire interior space of the structure (Fig. 2a). Further experiments studied the influence of the thickness of the air layer upon the thermal conductivity coefficient of the structures. For this purpose, all three types of insulating materials were arranged inside the structure in one layer (50 mm thick) and two layers (100 mm thick), leaving air gaps of 100 mm (Fig. 2c) and 50 mm thick (Fig. 2b), respectively. Additional structures using reed straws as insulating materials were formed with air gaps of 20 mm and 10 mm, respectively. RSs were arranged in the structure in an uncompressed state. VB foil

and GB interior face sheet were afterwards mounted with the sides using screws.

Table 1 presents the components of the experimental walls. Structures from S1 to S6 are considered reference samples because they use common heat insulation materials and they have low thermal conductivity coefficients around $0.04 \text{ W m}^{-1} \text{ K}^{-1}$. Eleven experimental wall structures with length \times width \times thickness of $600 \times 600 \times 174.5 \text{ mm}$ were designed and built for thermal conductivity measurements. Two replicates of each structure type were made and tested. The mean value of the thermal conductivity coefficient for each ΔT was calculated with the recorded results of the two replicate panels. The mean value of λ for each tested structure was calculated with recorded values of λ for the nine temperatures configurations of the test, according to Table 2. Before testing, the structures were conditioned for one week to the experimental environmental conditions.

Methods

The experimental walls were subjected to thermal conductivity coefficient (λ) measurements using the hot plate technique according to ISO 8301:1991 [27] and DIN EN 12667:2001 [28].

The HFM436 Lambda apparatus (Netzsch, Selb, Germany) was used for the test. The plate temperature of this equipment ranges between -20 and $70 \text{ }^\circ\text{C}$, and the calibration curves are incorporated into the program. Lambda apparatus is provided with an external cooler, it has 10 programmable data points, and it has maximum specimen thickness of 200 mm and length \times width of $610 \times 610 \text{ mm}$. It measures thermal conductivity ranging between 0.002 and $1.0 \text{ W m}^{-1} \text{ K}^{-1}$ with an accuracy of 1 to 3%. A Peltier system is used for plate temperature control. The method is based on the determination of the heat that passes from the hot plate to the cold plate through the tested material or structure. The temperatures of the two plates and the thermal conductivity coefficient which is calculated based on Fourier's Law are automatically recorded by the software of the apparatus. The equipment was calibrated according to the temperature configuration

shown in Table 2 before starting the measurement of the thermal conductivity coefficients.

The experimental walls were installed into the Lambda apparatus so that the exterior face (OSB 3) was always placed on the cold plate. Density was introduced as input data in the apparatus software. The densities of the experimental walls were calculated as the ratio between their masses and volumes. The samples were placed between two heated plates, set at different temperatures, according to Table 2. The heat flow through the sample is measured by a calibrated heat flux transducer. After reaching a thermal equilibrium, the test is done. The sample centre (250 × 250 mm) is used for the analysis. The heat flow meter method applied for measurement is a standardized test technique [27, 28]. A calibration measurement is first taken, and then, the Q-LAB software displays three graphs that give the operator a visual indication of test progress: thermal conductivity, ΔT and mean temperature.

Results and discussion

Thermal conductivity coefficient

The experiment simulates the outdoor temperature (T_1), which varies from negative temperatures (for cold season) to positive temperatures (for warm and hot seasons) and the indoor temperature (T_2), which is a constant at value of 20 °C. Thermal conductivity coefficients were determined for each ΔT and each mean temperature T_m . The mean values and standard deviations of the measured λ for each structure are presented in Fig. 3. Standard deviations were

Table 2 Temperatures configuration set-up

T_1 */°C	T_2 **°C	$\Delta T = T_2 - T_1$ /°C	$T_m = \frac{T_1+T_2}{2}$ /°C
- 10	20	30	5
- 5	20	25	7.5
0	20	20	10
5	20	15	12.5
10	20	10	15
15	20	5	17.5
25	20	- 5	22.5
30	20	- 10	25
35	20	- 15	27.5

*Bottom plate temperature

**Upper plate temperature

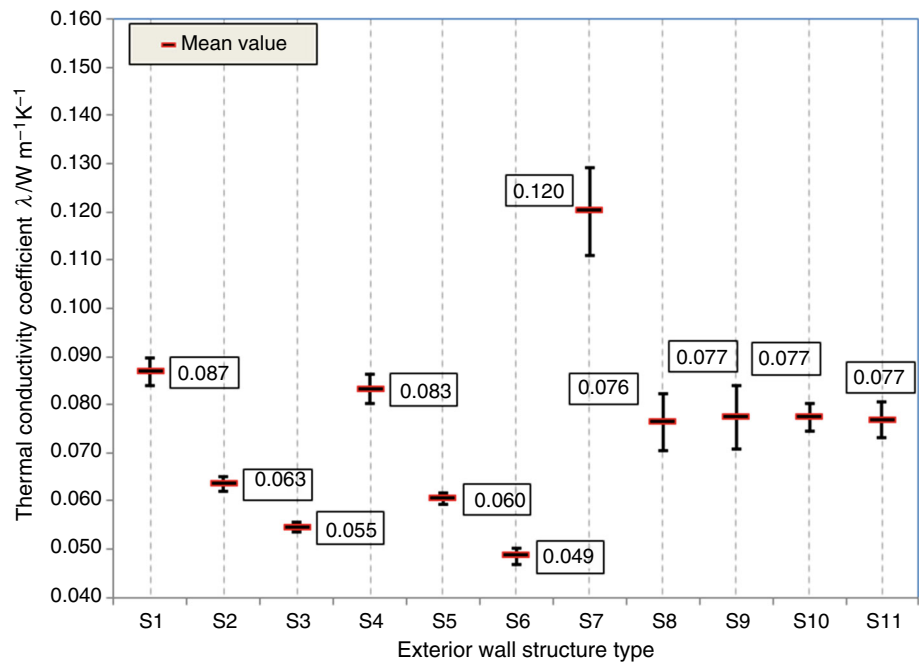
calculated for each structure considering all the recorded values of λ for the two replicates and for all ΔT configurations (entire test cycle). The results show that the lowest value of the thermal conductivity coefficient λ was recorded for three-layer (150 mm thick) RW insulation material (0.049 W m⁻¹ K⁻¹), followed by the wall structure having three layers of EPS heat insulation material (0.055 W m⁻¹ K⁻¹). All wall structures having RS as heat insulation material recorded higher values of λ than those of the similar structures with common heat insulation materials (RW and EPS).

The air layer with a thickness of 100 mm inside the wall structures favoured the occurrence of other phenomena such as heat transfer by convection and circulation of humid air with negative effects on the heat thermal insulation performance of the structure. These phenomena are

Table 1 Components of the experimental walls

Type of insulation material	Structures	Density ρ /kg m ⁻³	Thickness/mm						
			Interior face sheet GB	VB	Core layer				Exterior face sheet OSB 3
					Air	EPS	RW	RS	
Polystyrene (EPS)	S1	94.85	12.5	0.2	100	50	-	-	12
	S2	98.80	12.5	0.2	50	100	-	-	12
	S3	102.75	12.5	0.2	-	150	-	-	12
Rock wool (RW)	S4	99.14	12.5	0.2	100	-	50	-	12
	S5	107.39	12.5	0.2	50	-	100	-	12
	S6	115.63	12.5	0.2	-	-	150	-	12
Reed straws (RSs)	S7	113.29	12.5	0.2	100	-	-	50	12
	S8	135.68	12.5	0.2	50	-	-	100	12
	S9	158.07	12.5	0.2	-	-	-	150	12
	S10	149.11	12.5	0.2	20	-	-	130	12
	S11	153.59	12.5	0.2	10	-	-	140	12

Fig. 3 Mean values and standard deviations of the thermal conductivity coefficients measured for the tested structures during the entire test cycle



more pronounced in the case of reed structure, where the initial measured moisture content was of 11% and rise in temperature during the test led to water evaporation and increase in humidity in the air layer accompanied by the occurrence of heat transfer by convection. The result is a diminished thermal insulation capacity of this structure and a high mean value of λ , namely $0.120 \text{ W m}^{-1} \text{ K}^{-1}$ compared to $0.087 \text{ W m}^{-1} \text{ K}^{-1}$ for S1 (EPS as heat insulation material) and $0.083 \text{ W m}^{-1} \text{ K}^{-1}$ for S4 (RW as heat insulation material).

Reducing the thickness of the layer of air to 50 mm had as a result the improvement in thermal insulation capacity of all structures as follows: λ decreased by 28% for structures using EPS and RW and 38% for the structure using reed straws.

It has to be noticed that reducing the layer of air to 20 mm and 10 mm, respectively, in the case of wall structures with reed straws, the measured thermal conductivity coefficient λ remained almost constant around the value of $0.077 \text{ W m}^{-1} \text{ K}^{-1}$.

Considering the initial measured values of λ for RW ($0.04 \text{ W m}^{-1} \text{ K}^{-1}$), EPS ($0.042 \text{ W m}^{-1} \text{ K}^{-1}$) and RS ($0.054 \text{ W m}^{-1} \text{ K}^{-1}$), the performance of the wall structures proved to be similar to the performance of the insulation material expressed by its λ . Thus, knowing the thermal conductivity coefficients of the thermal insulation materials the behaviour of the structures is predictable.

The diagrams in Fig. 4 show different values of measured λ for various ΔT . The diagrams are split into two parts according to the temperature configuration set-up shown in Table 2. Thus, ΔT with values between -15 and

$10 \text{ }^\circ\text{C}$ corresponds to the summer temperatures, whilst the values of ΔT higher than $10 \text{ }^\circ\text{C}$ correspond to winter season. As seen in Fig. 4, the thermal conductivity coefficients have higher values for temperatures corresponding to summer season (on the left side). It can be explained by the increase in temperature and occurrence of water evaporation phenomenon along with the increase in humidity inside the air cavities. Those factors led to the increase in thermal coefficient values because of the more intense movement of the humid air and the occurrence of the convection phenomenon.

The temperature environment conditions at which the structures are more stable from the thermal insulation point of view are the negative temperatures, for which the values of λ are closer. The impact of negative temperatures on the structures causes the probable occurrence of condensation inside them, and this may favour the slower movement of the humidity, resulting in less variation of thermal conductivity coefficient.

The λ measurement protocol of the wall structures was set to a continuous temperature variation from negative to positive values so that the structures are subjected to successive cooling and heating, leading to variations of thermal conductivity coefficient λ . The structures were not removed from the equipment, passing an entire cycle during testing period of time.

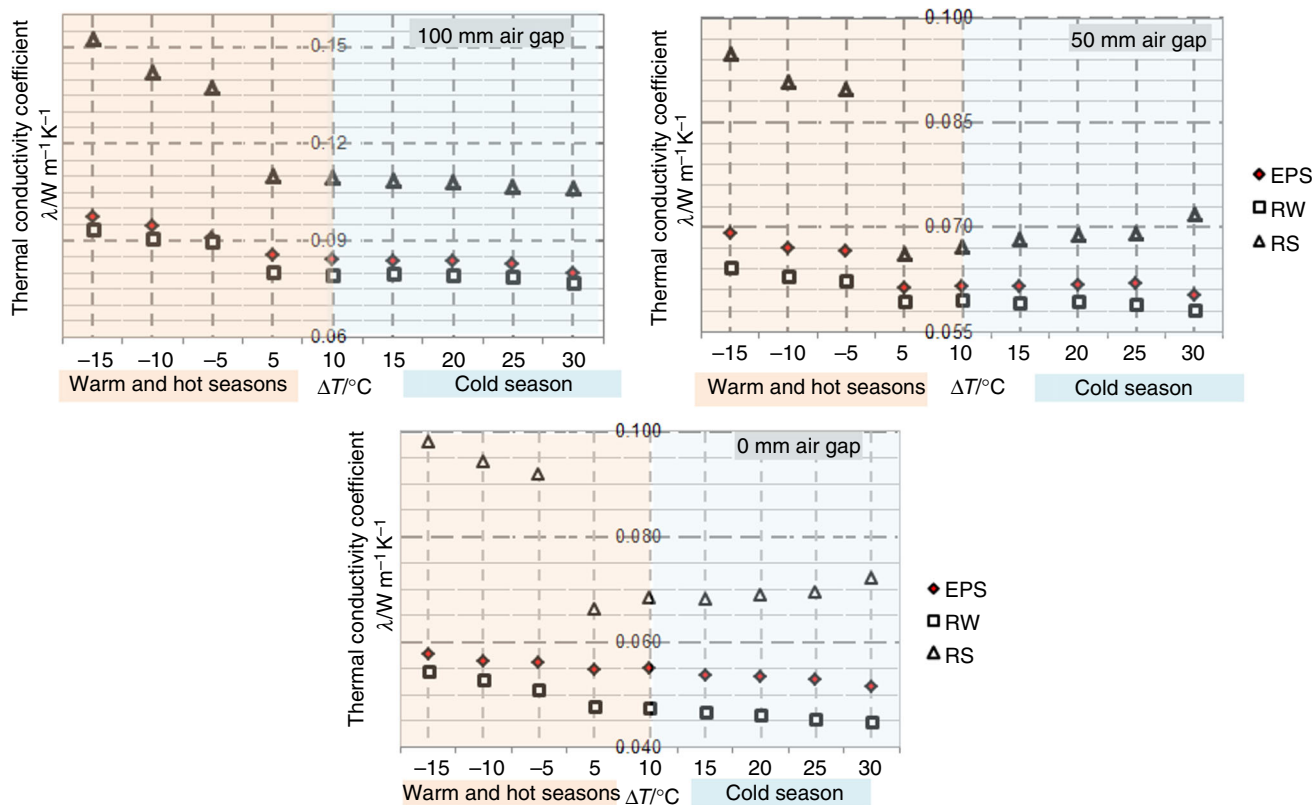


Fig. 4 Variation of thermal conductivity coefficient for similar wall structures with tested heat insulation materials: EPS, RW, RS

The influence of the air layer thickness in the case of reed straws wall structures

The graphical representation of the dependence between the thermal conductivity coefficient λ and the thickness of the air layer for wall structures with reed straws is shown in Fig. 5. As shown in Fig. 3, the mean values of thermal conductivity coefficients for this case are in a narrow range of values between 0.076 and 0.077 $W m^{-1} K^{-1}$ for air gaps up to 50 mm thicknesses. Analysing the behaviour of the thermal conductivity coefficient for wall structures with reed straws (Fig. 5), it can be observed that the narrowest

values in the range were recorded for the walls with the air layer thicknesses of 10 and 20 mm and for the structures without air gap. Broader values in the range of measured λ were recorded for air layer thicknesses of 50 mm and 100 mm, respectively. The higher values of λ were recorded for the case when the thermal resistance of the structure was influenced by the convection heat losses because of the high temperatures specific to summer conditions and to the movement of the humid air inside the structure, namely for the structures with 100 mm air gap. As the diagram in Fig. 5 shows, these phenomena are more reduced for the structures where no air gaps or air

Fig. 5 Variation of thermal conductivity coefficient λ against the thickness of the air layer for the structures with reed straws

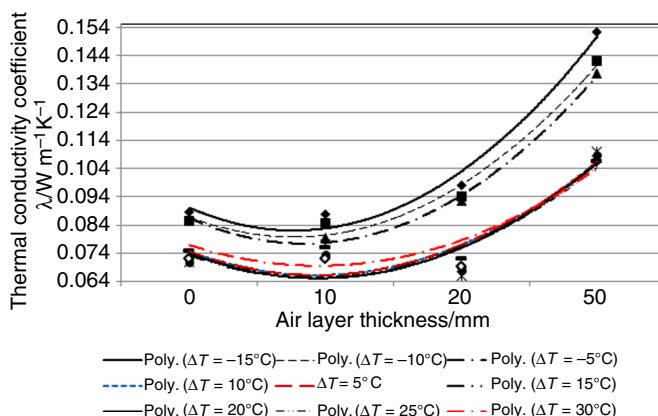


Table 3 Polynomial functions of λ against the air layer thickness inside the wall structure

$\Delta T/^\circ\text{C}$	$T_1/^\circ\text{C}$	$T_2/^\circ\text{C}$	Polynomial function (λ as a function of air layer thickness x)	R^2
30	- 10	20	$\lambda = 0.0042x^2 - 0.0184x + 0.0898$	0.77
25	- 5	20	$\lambda = 0.0048x^2 - 0.0214x + 0.0897$	0.79
20	0	20	$\lambda = 0.0049x^2 - 0.0221x + 0.0898$	0.79
15	5	20	$\lambda = 0.0048x^2 - 0.0211x + 0.088$	0.78
10	10	20	$\lambda = 0.0043x^2 - 0.0176x + 0.0835$	0.70
5	15	20	$\lambda = 0.0043x^2 - 0.0176x + 0.0835$	0.70
- 5	25	20	$\lambda = 0.009x^2 - 0.0444x + 0.1318$	0.93
- 10	30	20	$\lambda = 0.0091x^2 - 0.0443x + 0.1326$	0.93
- 15	35	20	$\lambda = 0.0101x^2 - 0.0492x + 0.1405$	0.93

thicknesses of 10 and 20 mm are present. The polynomial curves in Fig. 5 show a minimum point at an air gap of 10 mm. Figure 5 proposes a mathematical model to approximate the variation trend of λ . In fact, the experimental results for λ are not very far for air gaps up to 50 mm.

The polynomial variation of λ as a function of the air layer thickness (x) of the wall structures filled with reed straws is shown in Fig. 5, and the equations are given in Table 3, where the regression R^2 is between 0.70 and 0.79 for ΔT in the range between 5 and 30 °C and 0.93 for ΔT in the range of - 15 to - 5 °C. The weak fitting R^2 value for ΔT varying from 5 to 30 °C may be explained by collateral heat transfer phenomena that occurred when increasing the temperature of the lower plate from negative to positive values. After calibration, the lower plate reached a negative temperature of - 10 °C and the water inside the structure has frozen. With the increase in temperature, the water passed into the liquid phase and later in vapour phase, creating more numerous freely moving molecules and conferring internal mobility to water and vapours into the structure and occurrence of convective heat transfer in addition to conductive heat transfer, affecting thus the correlations with the pure conductivity phenomena.

The influence of the density on the thermal conductivity coefficient

The densities of the experimental wall structures are shown in Table 1 and Fig. 6. The highest values of the densities between 113.29 and 153.59 kg m⁻³ were recorded for the structures filled with reed straws.

Polynomial equations were found to predict the correlation between thermal conductivity coefficient and density of the structures (Fig. 6). The coefficient of determination (R^2) indicates that the predicted models completely fit for the structures filled with EPS and RW and the percentage of variations in the measured λ for the wall structures filled with RS indicates a good fit of the model.

Statistical ANOVA single-factor variance analysis was performed for the determination of the influence of the air layer thickness on the thermal conductivity coefficient value. The statistical analysis includes the mean values obtained in the experiment. Factors that significantly affect the thermal conductivity were determined using the reported p values. The thickness of the air layer was found to have a highly significant influence on the measured thermal conductivity at a 95% confidence level ($p \leq 0.05$) in the case of RW and EPS, whilst the air layer thickness in the case of RS was not statistically significant.

Conclusions

In this study, thermal conductivity of timber frame wall structures using reed straws as heat insulation materials was theoretically and experimentally investigated. Two directions were approached in the research: the first one was focused on comparing the thermal insulation capacity of reed straw (RS), as a renewable and natural resource, to that of common insulation materials such as RW and EPS; the second one investigated the influence of the wall air thickness on the performance of the thermal conductivity coefficient. With respect to the first direction, identical wall structures with RS, RW and EPS were made, tested and compared. The experimental results of λ showed best thermal performances for RW and EPS structures without air layer (0.049 and 0.055 W m⁻¹ K⁻¹, respectively), compared to similar RS structures (0.077 W m⁻¹ K⁻¹). Thermal conductivity ranged between 0.066 and 0.095 W m⁻¹ K⁻¹ for reed-filled wall structures. Similar results were recorded [4] for spruce bark (0.062 and 0.096 W m⁻¹ K⁻¹) or for straw bales 50 mm thick [10]. With regard to the second research direction, the present experimental study shows that with the increase in the air layer thickness inside RW and EPS structures, λ increases by approx. 15% for the thickness of 50 mm and around 60% for the thickness of 100 mm. Similar results as for RW and EPS structures were presented by other

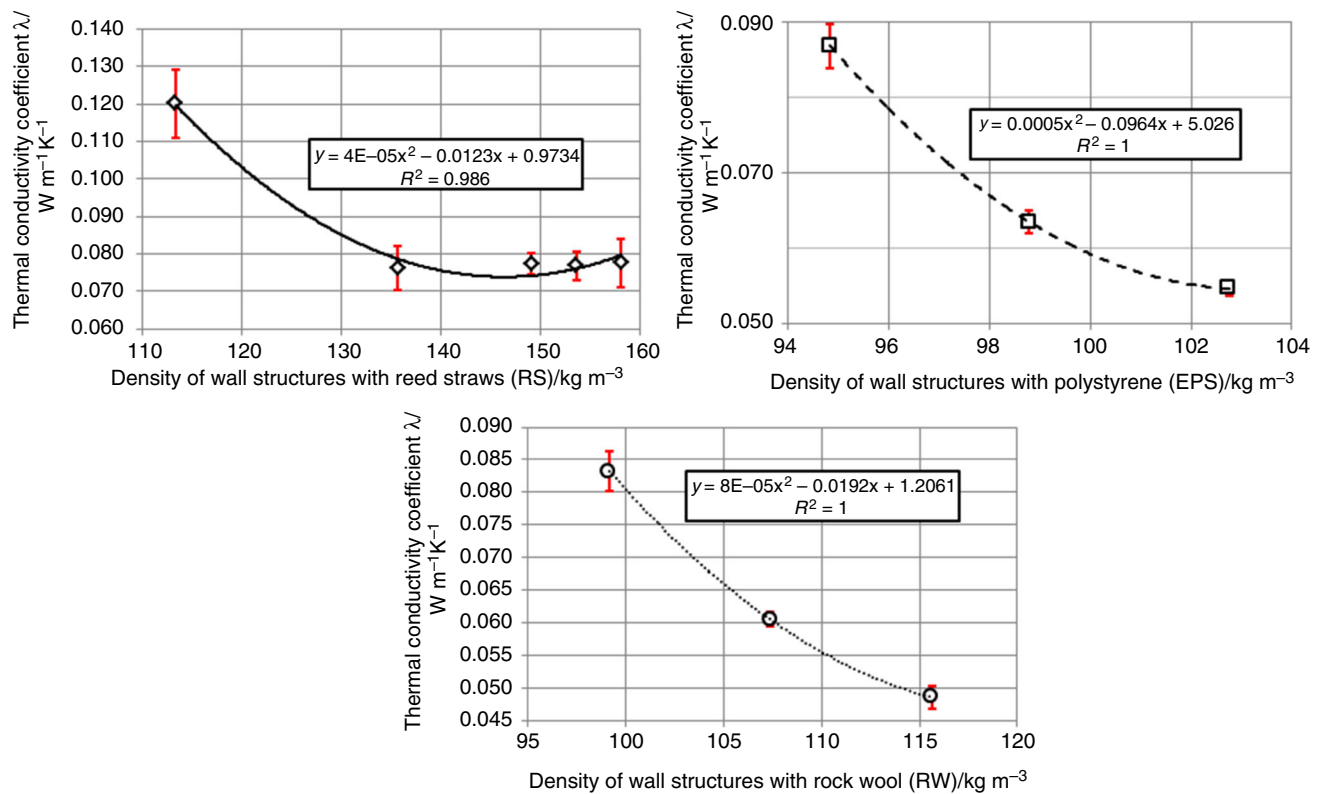


Fig. 6 Correlations between thermal conductivity coefficients and densities of the experimental wall structures

researchers [12] in case of using cellulose loose-fill material in the wood wall structure ($0.050 \text{ W m}^{-1} \text{ K}^{-1}$).

Less variation of thermal conductivity coefficient during the entire test cycle was reached by reed wall structures, for which λ was in the range of 0.076 to $0.077 \text{ W m}^{-1} \text{ K}^{-1}$ for the structures having the thicknesses of the air layer up to 50 mm . Instead, a value of $0.120 \text{ W m}^{-1} \text{ K}^{-1}$ was recorded for the structure with air layer thickness of 100 mm . The conclusion is that the same thermal performance is achieved by reed straws when the entire space inside the structures is filled with this material, or air gaps of 10 , 20 or 50 mm thicknesses are left in the structure. The same trend of good thermal performance when the air gap in the structure is thinner was observed by other researchers, too [11]. Lower thermal conductivity coefficients were registered by reducing the air layer thickness from 7 to 3 mm between the layers of paper that formed the interior structure of the wood frame wall. This was explained by the reduced impact of the convective heat transmittance that occurred in the air gaps. The ANOVA single-factor variance analysis performed in the present study shows that the air gap thickness is highly significant for the thermal conductivity in the case of RW and EPS, whilst the air layer thickness in the case of RS is not statistically significant.

The present study also shows that the variation of temperatures from negative to positive ones during the test cycle together with the occurrence of water evaporation phenomenon along with the increase in humidity inside the air cavities increases the thermal conductivity coefficient values because of the more intense movement of the humid air and convection occurrence, as shown in other studies [29–31]. This assumption confirms the lower heat insulation performance of all structures having 100 mm air gap thickness.

Polynomial equations were found to predict the correlation between thermal conductivity coefficient and density of the structures. The analysis of λ values in the case of reed wall structures had as a result equations of the polynomial functions for the dependence between the thermal conductivity and the thickness of the air layer. In order to complete the conclusions of the present study, further research is planned to provide detailed information on the heat transfer phenomena inside the structures, by measuring temperature and humidity along the thickness.

Acknowledgements The authors acknowledge the structural funds project PRO-DD (POS-CCE, O.2.2.1., ID 123, SMIS 2637, No. 11/2009) for providing the infrastructure used.

References

- Cao X, Liu J, Xilei D. Building energy-consumption status worldwide and the state-of-the-art technologies for zero-energy buildings during the past decade. *Energy Build.* 2016;128:198–213.
- Su X, Luo Z, Li Y, Huang C. Life cycle inventory comparison of different building insulation materials and uncertainty analysis. *J Clean Prod.* 2016;112(1):275–81.
- Asdrubali F, D'Alessandro F, Schiavoni S. A review of unconventional sustainable building insulation materials. *Sustain Mater Technol.* 2015;4:1–17.
- Kain G, Barbu CM, Hinterreiter S, Richter K, Petutschnigg A. Using bark as heat insulation material. *BioResources.* 2013;8(3):3718–31.
- Kain G, Lienbacher B, Barbu MC, Senck S, Alexander Petutschnigg A. Water vapour diffusion resistance of larch (*Larix decidua*) bark insulation panels and application considerations based on numeric modelling. *Constr Build Mater.* 2018;164:308–16.
- Brenci LM, Cosereanu C, Zeleniuc O, Georgescu SV, Fotin A. Thermal conductivity of wood with ABS waste core sandwich composites subject to various core modifications. *BioResources.* 2018;13(1):555–68.
- Miljan M, Miljan MJ, Miljan J, Akermann K, Karja K. Thermal transmittance of reed-insulated walls in a purpose-built test house. *Mires Peat* 2013/14;13(Article 07):1–12.
- Miljan M, Miljan J. Thermal transmittance and the embodied energy of timber frame lightweight walls insulated with straw and reed. In: IOP conference series: Materials Science Engineering, vol. 96; 2015. p. 012076. <https://doi.org/10.1088/1757-899x/96/1/012076>.
- Miljan MJ, Miljan M., Miljan J. Thermal conductivity of walls insulated with natural materials. In: 4th international conference civil engineering 13' proceedings, part I construction and materials, vol. 4; 2013. p. 175–79.
- Ashour T, Georg H, Wu W. Performance of straw bale wall: a case of study. *Energy Build.* 2011;43(8):1960–7. <https://doi.org/10.1016/j.enbuild.2011.04.001>.
- Pásztory Z, Horváth T, Glass SV, Zelinka SL. Thermal insulation system made of wood and paper for use in residential construction. *Forest Prod J.* 2015;65(7–8):352–7. <https://doi.org/10.13073/FPJ-D-14-00100>.
- Nicolajsen A. Thermal transmittance of a cellulose loose-fill insulation material. *Build Environ.* 2005;40(7):907–14. <https://doi.org/10.1016/j.buildenv.2004.08.025>.
- Zheng C, Li D, Ek M. Mechanism and kinetics of thermal degradation of insulating materials developed from cellulose fiber and fire retardants. *J Therm Anal Calorim.* 2018. <https://doi.org/10.1007/s10973-018-7564-5>.
- Samal S, Stuchlík M, Petrikova I. Thermal behavior of flax and jute reinforced in matrix acrylic composite. *J Therm Anal Calorim.* 2018;131(2):1035–40. <https://doi.org/10.1007/s10973-017-6662-0>.
- Jiang Y, Lawrence M, Hussain A, Ansell M, Walker P. Comparative moisture and heat sorption properties of fibre and shiv derived from hemp and flax. *Cellulose.* 2018. <https://doi.org/10.1007/s10570-018-2145-0>.
- Stevulova N, Estokova A, Cigasova J, Schwarzova I, Kacik F, Geffert A. Thermal degradation of natural and treated hemp hurds under air and nitrogen atmosphere. *J Therm Anal Calorim.* 2017;128(3):1649–60. <https://doi.org/10.1007/s10973-016-6044-z>.
- Roberts BC, Webber ME, Ezekoye OA. Development of a multi-objective optimization tool for selecting thermal insulation materials in sustainable designs. *Energy Build.* 2015;105(15):358–67. <https://doi.org/10.1016/j.enbuild.2015.07.063>.
- Kain G, Lienbacher B, Barbu M-C, Richter K, Petutschnigg A. Larch (*Larix decidua*) bark insulation board: interactions of particle orientation, physical–mechanical and thermal properties. *Eur J Wood Wood Prod.* 2018;76:489–98. <https://doi.org/10.1007/s00107-017-1271-y>.
- Labat M, Woloszyn M, Garnier G, Roux JJ. Dynamic coupling between vapour and heat transfer in wall assemblies: Analysis of measurements achieved under real climate. *Build Environ.* 2015;87:129–41.
- Durica P, Juras P, Gaspierik V, Rybarik J. Long-term monitoring of thermo-technical properties of lightweight constructions of external walls being exposed to the real conditions. *Procedia Eng.* 2015;111:176–82.
- Briga-Sá A, Nascimento D, Teixeira N, Pinto J, Caldeira F, Varum H, Paiva A. Textile waste as an alternative thermal insulation building material solution. *Constr Build Mater.* 2013;38:155–60. <https://doi.org/10.1016/j.conbuildmat.2012.08.037>.
- Vakili M, Karami M, Delfani S, Khosrojerdi S, Kalhor K. Experimental investigation and modeling of thermal conductivity of CuO–water/EG nanofluid by FFBP-ANN and multiple regressions. *J Therm Anal Calorim.* 2017;129(2):629–37. <https://doi.org/10.1007/s10973-017-6217-4>.
- Balaji N, Mani M, Venkatarama Reddy BV. Thermal performance of the building walls. In: Preprints of the 1st IBPSA Italy conference Free University of Bozen-Bolzano, vol. 346; 2013. p. 1–7.
- Bassiouny R, Ali MRO, NourEldeen E-SH. Modeling the thermal behavior of Egyptian perforated masonry red brick filled with material of low thermal conductivity. *J Build Eng.* 2016;5:158–64.
- Czajkowski Ł, Olek W, Weres J, Guzenda R. Thermal properties of wood-based panels: thermal conductivity identification with inverse modelling. *Eur J Wood Wood Prod.* 2016;74:577–84. <https://doi.org/10.1007/s00107-016-1021-6>.
- Kain G, Lienbacher B, Barbu MC, Plank B, Richter K, Petutschnigg A. Evaluation of relationships between particle orientation and thermal conductivity in bark insulation board by means of CT and discrete modelling. *Case Stud Nondestr Test Eval.* 2016;6:21–9.
- ISO 8301. Thermal insulation—determination of steady-state thermal resistance and related properties—heat flow meter apparatus. International Organization for Standardization, Geneva, Switzerland 1991.
- DIN EN 12667. Thermal performance of building materials and products—determination of thermal resistance by means of guarded hot plate and heat flow meter methods—products of high and medium thermal resistance. German Institute for Standardization, Berlin, Germany 2001.
- Bedane AH, Afzal MT, Sokhansanj S. Simulation of temperature and moisture changes during storage of woody biomass owing to weather variability. *Biomass Bioenergy.* 2011;35:3147–51.
- Bryś A, Bryś J, Ostrowska-Ligeza E, Kaleta A, Górnicki K, Glowacki S, Koczon P. Wood biomass characterization by DSC or FT-IR spectroscopy. *J Therm Anal Calorim.* 2016;126(1):27–35. <https://doi.org/10.1007/s10973-016-5713-2>.
- Modarresifar F, Bingham PA, Jubb GA. Thermal conductivity of refractory glass fibres. *J Therm Anal Calorim.* 2016;125(1):35–44. <https://doi.org/10.1007/s10973-016-5367-0>.

Publisher's Note Springer Nature remains neutral with regard to jurisdictional claims in published maps and institutional affiliations.